Submitted to the 1996 IEEE
Robotics and Automation Conference
Minneapolis, April 1996

Foot Placement and Velocity Control in Smooth Bipedal Walking

Eric R. Dunn   Robert D. Howe

Division of Applied Sciences
Harvard University
Cambridge, Massachusetts 02138
Tel. (617) 496-9098, Fax (617) 495-9837, Email eric@hrl.harvard.edu

Abstract

For a walking robot to negotiate rough terrain it must be able to adjust its step length to hit suitable footholds, and it must be able to regulate its forward speed. In this paper, we develop an algorithm to achieve these aims for a planar dynamic biped in the context of smooth exchange of support. The basis of the algorithm is a asymmetric gait to adjust velocity and a set of conditions which ensure smooth exchange of support. We tested our algorithm in simulation and on an experimental biped and found that the algorithm could track a 30% change in desired walking velocity and a 25% change in desired step length.

1 Introduction

Animals walk, vehicles roll. On prepared surfaces, wheels are smooth: they enable locomotion with minimal disturbance to the payload. This allows us to ride comfortably in automobiles at high speeds, so a "smooth ride" is a key attribute of a luxury car. Unfortunately, wheeled vehicles lose this ability to move smoothly when the ground is not regular, and on very rough terrain they cannot move at all. Here legged locomotion becomes a winning alternative, because it permits arbitrary placement of the foot to step on or over obstacles. Animals can move over extremely rugged terrain; the ability of goats to climb absurdly steep mountain sides is legendary, and humans routinely negotiate steep stairs and ladders. This motion is not smooth, however, even on level ground, since legged locomotion in many animals optimizes energy efficiency rather than smoothness [1].

Our research is aimed at understanding how to build robots that preserve the advantages of legs and simultaneously walk smoothly. In previous work, we considered the fundamental problem of smooth exchange of support for a simple planar bipedal robot. There we derived a set of conditions which ensure that the robot's body does not experience an instantaneous change in velocity as the robot's weight is transferred from one leg to the other. Here we consider methods to control other essential parameters of gait.

Hodgins [2] noted that in order for a legged robot to negotiate rough terrain, it must select a series of suitable footholds and then choose its step length to attain those footholds. During this process the robot must also regulate its forward speed. We propose an algorithm which permits the independent control of step length and walking velocity, while still satisfying the smooth exchange of support criteria to ensure that smooth locomotion is maintained. To investigate the efficacy of our new algorithm we examine its performance in simulation and on our experimental hardware.

Raibert, Hodgins, and their colleagues [2, 3, 4] examined the problems of foot placement and forward velocity control for their running robots. These remarkable machines can run, hop, negotiate stairsteps, and even somersault, but the objective of these machines is not smooth motion, and the running gaits they employ are not smooth. Kajita and his coworkers [5, 6] built a series of bipedal robots that minimize excursions of the robots' body, but their goal was to simplify the dynamics of the system, rather than create a smooth walk. Blajer and Schiehlen [7] have examined impact-free walking of a complex biped from a theoretical point of view. None of the foregoing studies have aimed at the the development of smooth walking over uneven ground.

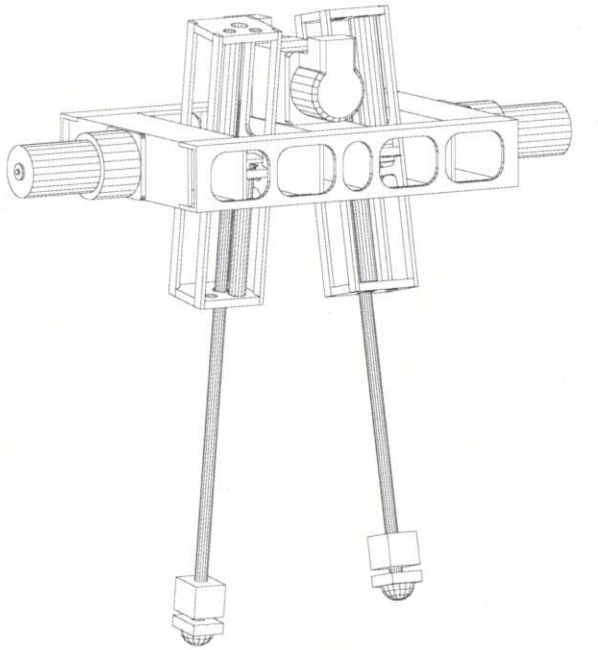

Figure 1: An experimental planar five-link walking biped.

2 Experimental hardware

We believe that experimental verification of our control strategies is essential, and, consequently, we have constructed a planar bipedal robot to serve as the test bed for our research. Figure 1 shows the machine's basic structure, which consists of a pair of legs joined to a body. Each leg pivots on a rotary hip joint at the body and contains a prismatic lower leg joint.

Pneumatic cylinders drive the extension and retraction of the lower legs. We selected pneumatic cylinders for this application because of their favorable force to weight ratio. Unfortunately, continuous control of pneumatic systems is notoriously difficult (see [8], for example), and we found it necessary to implement a nonlinear observer-based control scheme to obtain reasonable performance under walking conditions. The hip joints are driven by conventional DC servomotors with harmonic drive gearheads.

Force sensors near the hemispherical feet transduce ground reaction forces, and potentiometers at the joints permit measurement of the robot's configuration and orientation. The robot stands about 35 cm high and weighs approximately 5.6 kg. A boom mechanism constrains the motions of the robot to the sagital plane, simplifying the problem of balance and eliminating out of plane considerations.

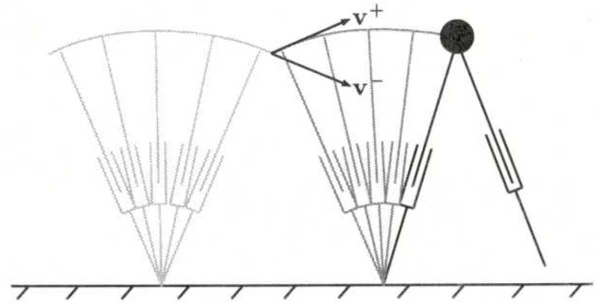

Figure 2: The compass gait. During single support, the hip follows the arc of a circle with radius equal to the stance leg length. At exchange of support, there is an instantaneous change in linear velocity of hip.

3 Smoothing bipedal walking

A step in the gait of a dynamic biped consists of two phases: *(a)* a single support phase in which one leg is in contact with the ground and the other leg is not, and *(b)* an exchange of support during which the legs trade roles. In the single support phase, the *stance leg* is in contact with the ground and carries the weight of the biped, while the *swing leg* usually swings forward in preparation for the next step. At exchange of support the weight of the robot is transferred from one leg to the other. In this section, we examine exchange of support, discuss why it might not be smooth, and, present of set of constraints which ensure smooth exchange of support.

Inman *et al.* [9] examined bipedal walking in humans and proposed a model of bipedal walking based on the compass gait (Figure 2). In this gait the leg lengths are fixed, so the hip trajectory follows the arc of a circle as the biped pivots about the distal end of the stance leg. At exchange of support, the stance and swing legs trade roles, and the hip begins to trace an arc of a new circle. Because the origins of the two circles are not coincident, the hip trajectory contains a cusp at exchange of support. Velocity vectors $\mathbf{v}^-$ and $\mathbf{v}^+$ attached to the hip trajectory at a cusp indicate linear velocity of the hip just before and just after exchange of support, respectively. The two velocities are not equal ($\mathbf{v}^- \neq \mathbf{v}^+$), and the hip experiences an instantaneous change in velocity at exchange of support. A payload or passenger riding at the hip of the biped would experience this instantaneous change in velocity as an infinite acceleration with an accompanying infinite impulsive force. We see, in this case, that the compass gait is certainly not smooth.

If we have control of the lengths of the legs, however, we can modify the compass gait to ensure smooth

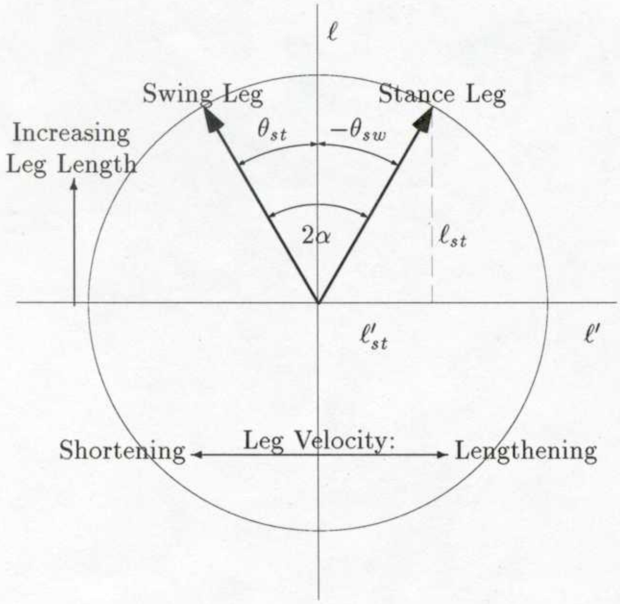

Figure 3: Phase diagram for smooth exchange of support. The diagram illustrates the relationship between the necessary stance and swing legs motions.

exchange of support. Specifically, we require that the velocity of the hip remains unchanged during exchange of support

$$\mathbf{v}^- = \mathbf{v}^+,$$

and then determine the leg lengths and velocities necessary to satisfy this condition. The authors presented a complete derivation of these conditions in a previous paper [10] and only summarize the results here.

Defining the terms of interest, let ℓ_{st} be the length of the stance leg, ℓ_{sw} be the length of the swing leg, θ_{st} be the angle of the stance leg with respect to gravity, θ_{sw} be the angle of the swing leg with respect to gravity, and let 2α be the angle between the legs ($2\alpha = \theta_{st} - \theta_{sw}$). With these definitions, the conditions for smooth exchange of support with no velocity discontinuity are

$$\begin{bmatrix} \ell'_{sw} \\ \ell_{sw} \end{bmatrix} = \begin{bmatrix} \cos 2\alpha & -\sin 2\alpha \\ \sin 2\alpha & \cos 2\alpha \end{bmatrix} \begin{bmatrix} \ell'_{st} \\ \ell_{st} \end{bmatrix}, \quad (1)$$

$$\ell'_{st} + \ell_{st} \tan \theta_{sw} = 0, \quad (2)$$

where $(\cdot)'$ indicates a derivative with respect to θ_{st}.

To illustrate the geometrical meaning of Equations (1, 2), we use a phase diagram (Figure 3). The vertical axis in Figure 3 is leg length, and the horizontal axis is rate of change of leg length. In this diagram the length and rate of change of each leg is represented by a vector. From Equation (1), the relationship between legs' vectors is a simple rotation by 2α. Equation (2) fixes the angle of the stance leg's vector with respect to the vertical axis.

The significance of the phase diagram is that it shows the lengths and rate of change of the legs during exchange of support. For the particular "symmetric" configuration in Figure 3 we see that $\theta_{st} + \theta_{sw} = 0$. Since the leg vectors lie on a circle, the legs must be the same length at exchange of support. The rate of length change of the legs are equal but opposite, with the stance leg extending and the swing leg retracting. These coordinated actions eliminate any velocity discontinuity of the hip at exchange of support.

The phase diagram does not completely fix all parameters at exchange of support. In particular, the radius of the circle is a free parameter, allowing us to select the body height at exchange of support. The angle 2α is free which allows us to specify step length. Finally, either θ_{st} or θ_{sw} may be freely selected. We will use this degree of freedom to control the forward walking velocity of the biped.

4 Velocity control with asymmetry

Using a technique similar to the velocity control algorithm employed by Raibert [3] on his hopping robots, we seek to control the forward velocity of our walking robot by introducing an asymmetry to the walking gait. We define a gait asymmetry β as the difference between the stance leg angle and the swing leg angle at exchange of support,

$$\beta = \theta_{st} - (-\theta_{sw}).$$

When the gait is symmetric as in Figure 3, the stance phase begins with the body a particular distance behind the point of support, and ends with the body the same distance in front of the point of support. The body spends equal amounts of time in front of and behind the point of support, and the net acceleration due to gravity acting on the body is zero.

If we introduce a positive asymmetry to the gait, then θ_{st} increases, $-\theta_{sw}$ decreases, and the biped's body will spend less time behind the point of support than in front of it. Gravity will have more opportunity to accelerate than decelerate the body, and the result will be a net step-to-step acceleration. Conversely, a negative asymmetry will result in a net deceleration from step-to-step.

Since asymmetry in the gait produces velocity changes, our control algorithm closes a feedback loop

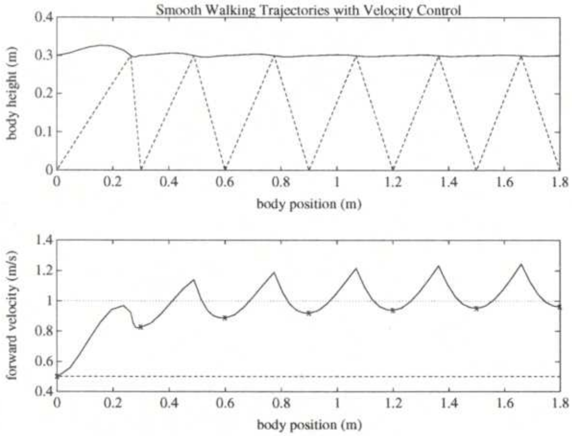

Figure 4: Velocity control algorithm applied to a biped in simulation. The upper plot shows the hip position and the location of the stance and swing legs at exchange of support. The biped walks in the positive x direction. The lower plot shows the forward velocity of the robot. The robot begins with a forward velocity of 0.5 m/s. The desired velocity is 1.0 m/s.

around forward velocity by setting the asymmetry proportional to the velocity error, $\beta = G(v_d - v)$, where v_d is the desired velocity, v is the measured walking velocity and G is a feedback gain. With the asymmetry selected on the basis on velocity error, and step length L and body height h specified by an operator, the algorithm must solve the smooth exchange of support conditions consistent with the desired values for β, L, and h. The solution process is straightforward once a value for θ_{st} is found from the equation

$$\tan\theta_{st} + \tan(\theta_{st} - \beta) = \frac{L}{h}.$$

This equation is readily solved online with a few iterations of Newton's method from the symmetric initial conditions $\theta_{st_0} = \tan^{-1}(\frac{L}{2h})$.

5 Implementations

To test the velocity and step length control algorithms developed in the previous section, we implemented the controller in simulation and on the experimental biped.

5.1 Simulation

For the purposes of simulation, we modeled the biped as an inverted pendulum with adjustable leg length. The model neglected body and swing leg dynamics and also assumed that the leg lengths and swing hip angle could be controlled exactly. In operation, the simulation begins with the body moving over the point of support with some initial velocity. With the body over the point of support, the velocity control algorithm compares the forward velocity to the desired forward velocity and computes a gait asymmetry based on the velocity error. Based on this asymmetry, the body height, and the desired step lengths, the smooth exchange of support conditions are applied to obtain θ_{st}, θ_{sw}, and the required leg lengths and velocities. A cubic spline trajectory is computed to drive the stance leg length to its target value, and then the model is integrated forward to exchange of support.

At exchange of support, the swing leg position and velocity are known, and are assigned to the new stance leg. A second cubic spline is computed for the stance leg length program, and the model is integrated forward to a point where the body is again over the point of support. At this stage one step is complete, and the simulation process repeats for additional steps.

In Figure 4 we show the results of one simulation. Here the robot begins with a forward velocity of 0.5 m/s and we ask that it accelerate to 1.0 m/s. In accordance with the velocity control algorithm, the gait begins with a large positive asymmetry, and the robot accelerates rapidly. By the midpoint of the second step (step midpoints are indicated by small x's in Figure 4), the forward velocity is greater than 0.8 m/s. On subsequent steps the forward velocity converges to the desired velocity, and the gait becomes more symmetrical.

An examination of the second plot in Figure 4 illustrates the effect of smooth exchange of support constraints. In this plot, we see that forward velocity is continuous across each exchange of support, as we required. We also note, however, that the velocity trajectory contains a cusp. That is, the *acceleration* is discontinuous. The origin of this discontinuity is easy to understand. Just before exchange of support the point of support is behind the body and the body accelerates. Just after exchange of support the point of support is in front of the body and the body decelerates. Hence, our exchange of support conditions provide sufficient smoothing to eliminate infinite accelerations, but do not eliminate infinite *jerk*.

5.2 Experimental Implementation

To test our velocity and step length control algorithm on the experimental biped, we constructed a control panel from which an operator could adjust the

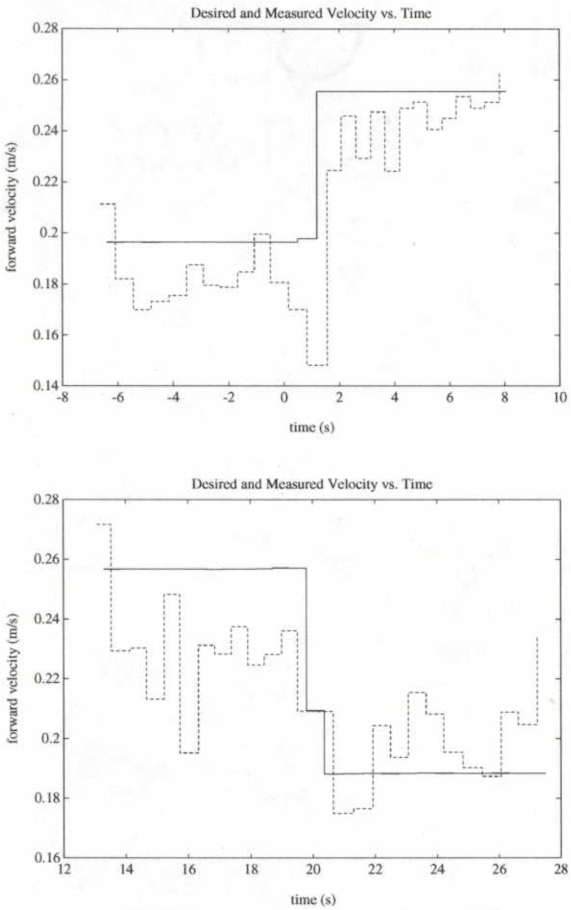

Figure 5: Velocity control algorithm applied to the experimental biped. The solid line is the desired forward velocity. The dashed line is the estimated forward velocity at each step.

value of desired step length or velocity while the robot walked. In the first of three experiments, the operator began with one desired speed and then increased the desired walking speed halfway through the walk. In the second experiment the operator decreased the desired walking speed during the walk. In the final experiment the operator adjusted the step length of the robot.

Figure 5 plots data taken from the first two experiments. In the first experiment, the initial desired velocity is 0.195 m/s. For the first dozen steps of the walk, the robot maintains a forward speed near the desired velocity. When the operator increases the walking speed by 30% to 0.257 m/s in the middle of the thirteenth step, the robot stumbles slightly, but then accelerates to near the new desired value. The step-to-step speed variation present in the data even when

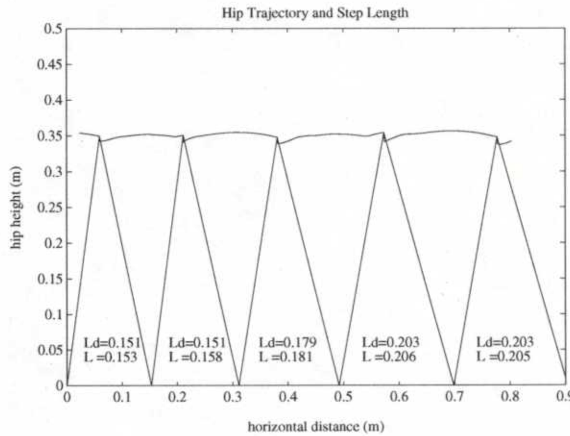

Figure 6: Hip trajectory and step length during a walk. The hip height shows some periodic variation around its nominal value of 0.35 m. The positions of the stance and swing legs at each exchange of support are shown. The actual step length L is compared with the desired step length L_d. All lengths are in meters.

the operator commands a constant velocity is typical of this robot, and we believe that it is due primarily to joint control errors in the pneumatic legs.

The second plot in Figure 5 plots data from the second experiment, in which the operator decreases the desired velocity during the walk. We see that the robot's velocity decreases in response to the command, again with considerable step-to-step variation.

We present data from the third experiment in Figure 6. In this experiment the operator increases the desired step length from about 0.15 m to 0.20 m during the walk. Since step length in just a kinematic condition in the algorithm, we expect the actual step length to track the desired step length very closely. The data upholds this expectation and we see the step length errors during the walk are just a few percent of the total step length, with the largest error being 7 mm.

Also shown in Figure 6 are the hip trajectories across five steps. At exchange of support, the hip appears to sag by as much as 5 mm, despite our efforts to smooth the exchange of support. When the weight of the body in transferred to the new stance leg, the pressure in the pneumatic cylinder must increases rapidly. We believe the hip sag is a result of saturation in the pneumatic valve as it tries to raise the pressure in the leg.

6 Conclusions

We have developed a control algorithm which can independently regulate the step length and velocity of a bipedal gait, in the context of smooth exchange of support. The importance of this algorithm is that it enables the development of dynamic bipedal walkers which can walk smoothly while negotiating rough terrain. In future work, we will apply the control scheme to rough terrain problems.

In simulating the algorithm, we found that it is successful, but with limits on the achievable smoothness. In experiments we again found that the algorithm is successful, but its authority and smoothness are limited by joint control errors. Future work will address these deficiencies by the inclusion of an explicit double support phase.

References

[1] R. McN. Alexander. The gaits of bipedal and quadrupedal animals. *International Journal of Robotics Research*, 3(2):49–59, Summer 1984.

[2] J. Hodgins. Legged robots on rough terrain: experiments in adjusting step length. In *Proceedings of the IEEE International Conference on Robotics and Automation*, 1988.

[3] M. H. Raibert. *Legged Robots that Balance.* MIT Press, Cambridge, 1986.

[4] J. K. Hodgins and M. H. Raibert. Biped gymnastics. *International Journal of Robitics Research*, 9(2):115–132, April 1990.

[5] S. Kajita, T. Yamaura, and A. Kobayashi. Dynamic walking control of a biped robot along a potential energy conserving orbit. *IEEE Transactions on Robotics and Automation*, 8(4):431–438, August 1992.

[6] S. Kajita and K. Tani. Study of dynamic biped locomotion on rugged terrain. In *Proceedings of the IEEE International Conference on Robotics and Automation*, pages 1405–1411, April 1991.

[7] W. Blajer and W. Schiehlen. Walking without impacts as a motion/force control problem. *Journal of Dynamics Systems, Measurement, and Control*, 114:660–665, December 1992.

[8] S. Liu and J. E. Bobrow. An analysis of a pneumatic servo system and its application to a computer-controlled robot. *ASME Journal of Dynamic Systems, Measurement, and Control*, 110:228–235, September 1988.

[9] V. T. Inman, H. J. Ralston, and F. Todd. *Human Walking.* Williams & Wilkins, Baltimore, 1981.

[10] Eric R. Dunn and Robert D. Howe. Towards smooth bipedal walking. In *Proceedings of the IEEE International Conference on Robotics and Automation*, volume 3, pages 2489–2494, San Diego, May 1994.